Carburization effects on pig iron nugget making

B. Anameric, K.B. Rundman and S.K. Kawatra
Graduate student, Dept. of Chemical Engineering; professor, Dept. of Materials Science and Engineering; and professor, Dept. of Chemical Engineering, respectively, Michigan Technological University, Houghton, Michigan

Abstract
The iron nugget process is an economical, environmentally friendly, cokeless, single-step pig iron making process. Residence-time dependent process requirements for the production of pig iron nuggets at a fixed furnace temperature (1,425°C) were investigated. Depending on the residence time in the furnace, three chemically and physically different products were produced. These products were direct reduced iron (DRI), transition direct reduced iron (TDRI) and pig iron nuggets (PIN). The increase in the carbon content of the structure as a function of residence time was detected by optical microscopy and microhardness measurements. Sufficient carbon dissolution for the production of pig iron nuggets was obtained after a residence time of 40 minutes. The pig iron nuggets produced had chemical and physical properties similar to blast furnace pig iron. They were liquid-state products, and the slag was completely separated from the metal.

Key words: Pig iron nuggets, Direct reduced iron, Transition direct reduced iron, Carburization

Introduction
Blast furnace technology is still the primary method for pig iron production. The schematic process flowsheet and requirements are shown in Fig. 1. The success of this process is dependent on the quality of the raw materials used. Production or reliable supply of high-quality raw materials such as sinter, pellets and coke are the primary economical and environmental constraints of the process (Zervas et al., 1996a, 1996b, 1996c and 1996d). In addition, the inflexibility of the process capacity, the high capital and operating costs and the energy lost between steps led to a search for alternatives, such as the iron nugget process (Anameric and Kawatra, 2004).

The iron nugget process (Kobe Steel's ITMk3 process) is an economical, environmentally friendly, cokeless, single-step pig iron making process (Anameric and Kawatra, 2004). The schematic process flowsheet and requirements are shown in Fig. 2. The advantages of the iron nugget process can be summarized as follows:

- Environmental drawbacks of the blast furnace process are reduced by using widely available coal instead of coke.
- Lower capital and operational costs because all the infrastructure and auxiliary plants required for the blast-furnace process are not needed (Figs. 1 and 2), and coal is less expensive than coke.
- Energy conservation due to utilization of dried green balls instead of indurated (heat hardened) pellet or sinter (Figs. 1 and 2).
- Highly metallized, solid, slag free, high-density pig iron nuggets are produced using a single-step process. These nuggets are chemically comparable to blast-furnace pig iron, and they are both stable and easy to handle.

One of the drawbacks of using pig iron nuggets is that they need to be remelted for use in basic oxygen furnace steelmaking. However, they can be used in electric arc furnace steelmaking or in ferrous foundry operations without the need for premelting. In addition, if pig iron nuggets were used in an electric arc furnace instead of direct reduced iron, the energy consumption for steelmaking would be lowered because the slag is already removed from the structure and does not need to be melted along with the metal. Utilization of pig iron nuggets in the electric arc furnace instead of steel scrap is also more beneficial because nuggets have a better-known chemical composition.

One of the most important features of the iron nugget process is the separation of impurities from the metal by formation of fusible slag. Slag separation can only be achieved after the formation of two immiscible liquid phases, metal and slag. During the reduction of magne-

Paper number MMP-05-005. Original manuscript submitted online August 2005. Revised manuscript accepted for publication January 2006. Discussion of this peer-reviewed and approved paper is invited and must be submitted to SME Publications Dept. prior to Feb. 28, 2007.

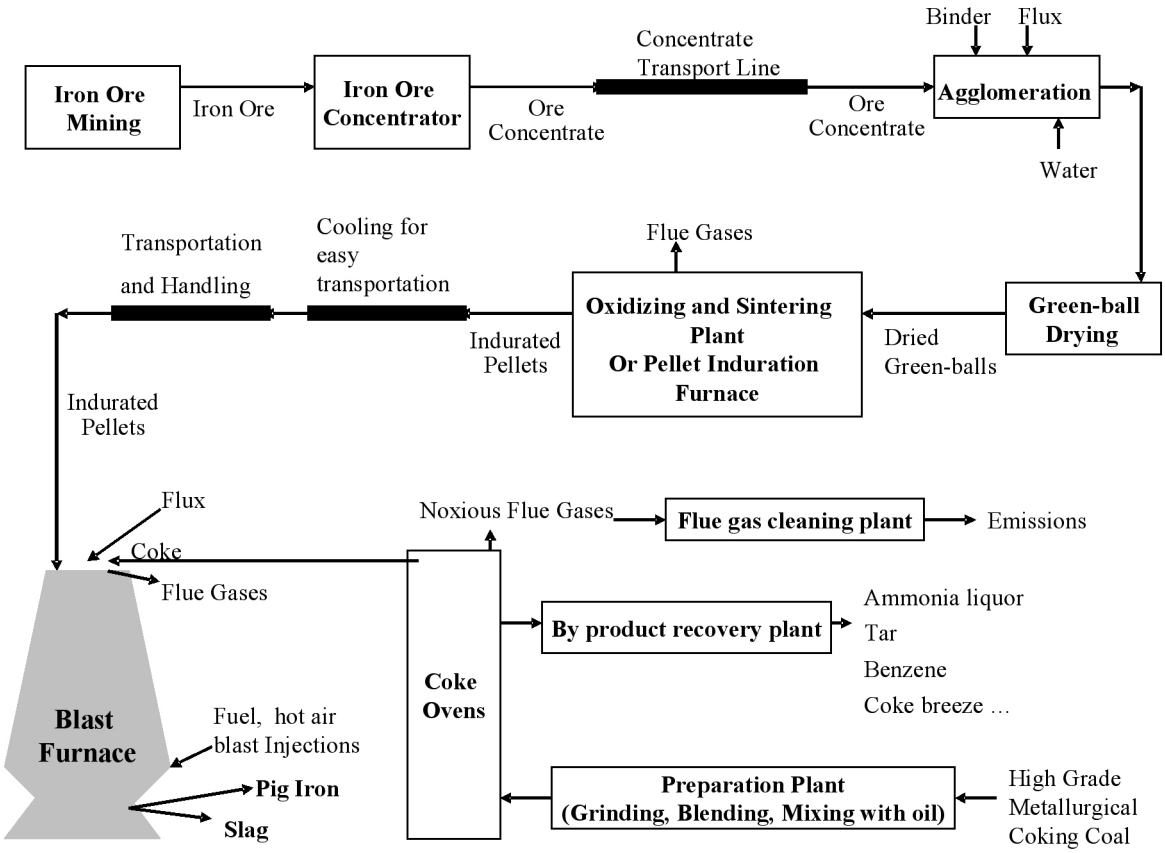

Figure 1 — The schematic process flowsheet and requirements of blast furnace process.

tite to pure iron, slag-forming reactions take place. The slag formed melts at a lower temperature (around 1,200°C) than the 1,535°C needed for the pure iron produced during the initial stages of solid-state reduction. Carburization of the pure iron is required for lowering its melting temperature and obtaining a melt and slag separation at molten state.

The carburization requirements for the production of liquid-state product (pig iron nuggets) and slag separation were investigated at a constant furnace temperature of 1,425°C. This temperature was selected because, based on previous work, it is near the minimum temperature needed to produce pig iron nuggets (Anameric and Kawatra, 2004). For this purpose, the dried green balls bearing coal and limestone were fired at the following furnace residence times: 10, 16, 22, 28, 30, 34, 40, 50 and 60 minutes. The resulting products were characterized according to their state after heat treatment, their microstructure and their microhardness. The observations of the state of the products after heat treatment were carried out as a preliminary method for the determination of the sequence of events leading to melting and slag separation. The microstructural investigation was carried out to determine the state of formation, phases present and presence of carbon in the structure. The microhardness measurements were carried out to determine the change in the carbon content. This method was chosen because the microhardness increases with increased carbon content (Krauss, 1990).

Theoretical background

Pig iron nugget making. During firing of dried green balls, the following events take place that result in iron nugget formation: thermal decomposition of coal, reduction, slag formation, carburization, iron melting and slag separation.

Generalized pertinent nugget-forming reactions can be given as follows (Chatterjee, 1994; Haque and Ray, 1995; Zervas et al., 1996; Nascimento et al., 1997, 1998, 1999):

$$\text{Coal} \rightarrow CO, CO_2, H_2, N_2, C_nH_m, C \quad (1)$$

$$C + O_2 \leftrightarrow CO_2 \quad (2)$$

$$CO_2 + C \leftrightarrow 2\,CO \quad (3)$$

$$C + \tfrac{1}{2}\,O_2 \leftrightarrow CO \quad (4)$$

$$CH_4 + CO_2 \leftrightarrow 2CO + 2H_2 \quad (5)$$

$$C + H_2O \leftrightarrow CO + H_2 \quad (6)$$

$$Fe_3O_4 + C \leftrightarrow 3FeO + CO \quad (7)$$

$$FeO + C \leftrightarrow Fe + CO \quad (8)$$

$$Fe_3O_4 + CO \leftrightarrow 3FeO + CO_2 \quad (9)$$

$$FeO + CO \leftrightarrow Fe + CO_2 \quad (10)$$

$$Fe_3O_4 + H_2 \leftrightarrow 3FeO + H_2O \quad (11)$$

$$FeO + H_2 \leftrightarrow Fe + H_2O \quad (12)$$

$$CaCO_3 \leftrightarrow CaO + CO_2 \quad (13)$$

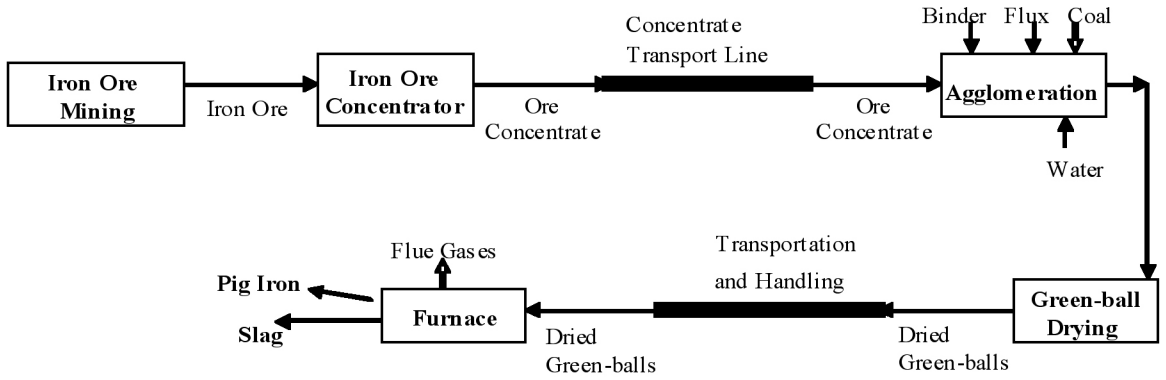

Figure 2 — The schematic process flowsheet and requirements of iron nugget process.

$$CaO + SiO_2 \leftrightarrow CaSiO_3 \quad (14)$$

$$SiO_2 + 2C \leftrightarrow Si + 2CO \quad (15)$$

$$FeO + SiO_2 \leftrightarrow FeSiO_3 \quad (16)$$

$$FeSiO_3 + CaO \leftrightarrow CaSiO_3 + FeO \quad (17)$$

$$FeS + CaO + CO \leftrightarrow CaS + FeO + CO \quad (18)$$

$$3Fe + C \leftrightarrow Fe_3C \quad (19)$$

Some of these reactions are exergonic — they have Gibbs free energy changes less than zero at high temperatures. As a result, they proceed spontaneously. Some of these reactions are energonic — they have Gibbs free energy changes higher than zero at high temperatures. As a result, these reactions are nonspontaneous.

Thermal decomposition of coal (Reaction (1)) and reducing gas regeneration reactions, represented by Reactions (2) through (6), take place in the same reactor in which the iron nuggets are produced. This eliminates the need for other reactors for the gasification, gas quenching, gas regeneration and gas heating. Reaction (3) of the reducing gas regeneration reactions is an important reaction known as Boudouard reaction. This reaction was found to be the rate-controlling step for iron ore reduction according to Rao (1971), Fruehan (1977), Seaton et al. (1983), Srinivasan and Lahiri (1977), Abraham and Ghosh (1979) and Mourao and Capocchi, (1996).

The endothermic, exergonic direct reduction reactions, through which solid carbon reacts with solid magnetite (Fe_3O_4) and wustite (FeO), are represented by Reactions (7) and (8). The endothermic, exergonic indirect reduction reaction, where the gas products of direct reduction (Reactions (7) and (8)) or the reducing gas forming reactions (Reactions (1), (3), (4), (5) and (6)), i.e., carbon monoxide, react with solid magnetite (Fe_3O_4), is represented by Reaction (9). The exothermic, energonic indirect reduction reaction, where carbon monoxide reacts with wustite (FeO), is represented by Reaction (10). This reaction was found to be the rate-controlling step for iron ore reduction according to Ghosh and Tiwari (1970), Srinivasan and Lahiri (1977), Mourao and Capocchi (1996). Other endothermic, energonic reduction reactions, where hydrogen is the reducing agent, are represented by Reactions (11) and (12).

Some of the important slag-forming reactions are represented by Reactions (13) through (18). Due to the complexity and inhomogeneity of the slag system, some less-important reactions are excluded.

After the reduction of the iron ore (magnetite) according to Reactions (7) through (12), the carbon diffusion, Reaction (19), into the metal lowers the melting temperature of the metal (this occurs until the eutectic composition is reached). The temperature versus carbon-composition stability diagram is shown in Fig. 3. Slag separation can only be achieved after the formation of two immiscible liquid products: slag and metal. These liquids separate due to differences in density and to surface tension effects.

The kinetics of these reactions is enhanced by agglomeration of an iron ore source, flux and reductant/carburizor together. The close contact of the reacting materials and the availability of a large number of reacting sites enhance the direct reduction and slag-forming reactions. Also, the internal gas generation and small diffusion distances in the agglomerated mixture enhances the indirect reduction reactions, reducing gas regeneration, slag forming and carburization reactions (Goksel ,1977; Goksel et al., 1988; Goksel et al., 1991; Mourao and Capacchi, 1996; Nascimento et al., 1998; Agrawal et al., 2000)

White cast iron. Once the magnetite reduces to iron, carbon gradually dissolves into the metal, resulting in melt formation. The cooling of this melt forms one of the several cast iron structures. Comparison of pig iron nugget structure with cast iron structures that form under different conditions gives information about composition and thermal history. It was previously determined that the pig-iron nuggets have a structure that closely corresponds to white cast iron.

The cast irons are a class of ferrous alloys with a carbon content of 2% to 4% and a silicon content of 1% to 3% in addition to other alloying elements (Smith, 1993). It can be estimated from Fig. 3 that alloys with this carbon composition range become completely liquid at temperatures between approximately 1,150° and 1,425°C. Cast irons solidify as heterogeneous alloys and always have more than one phase and microconstituent in their microstructure. During solidification of iron-carbon alloys, the carbon is distributed in solid solution in austenite and the eutectic product of either cementite (Fe_3C) or graphite.

Microstructural examination is the most effective technique for the identification of cast irons. This examination is based on the form and shape in which the major portion of the carbon occurs in the iron. Chemical analysis is not definitive in identifying the various types of cast irons because the chemical compositions overlap as shown in Table 1.

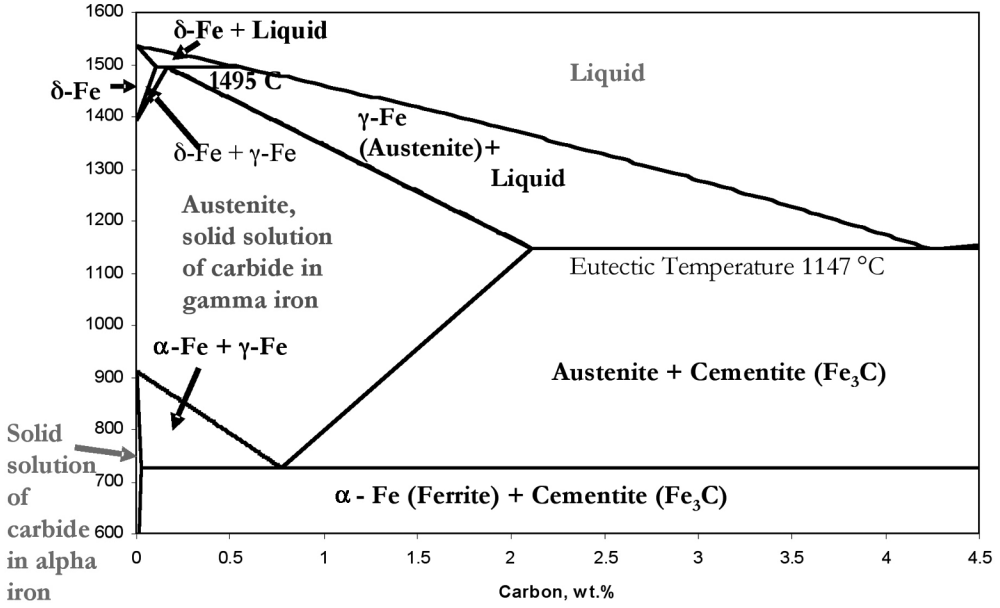

Figure 3 — A portion of the iron-carbon metastable phase diagram (Callister, 1997; Smith, 1993).

If for a low-silicon cast iron (less than 1.0% by weight Si) the carbon in the molten iron remains combined with iron in the form of iron carbide (cementite) it is called white cast iron (see Fig. 4). The chemical composition of the white cast iron compared to blast furnace pig iron is shown in Table 1. Throughout this research, microstructural examination was used for identification of white cast iron, which has a comparable chemical composition with blast furnace pig iron.

The white cast iron microstructure (Fig. 4) does not contain free graphite as does gray iron, malleable iron, or ductile iron. The fracture surface of this alloy appears white. In Fig. 4 the dark gray areas represent the dendritic grains of austenite that formed first on cooling (Fig. 3). Austenite dendrites transform by nucleation and growth to pearlite (alternating layers of Fe_3C and α-ferrite) under equilibrium-cooling conditions. In Fig. 4 light areas represents the eutectic iron carbide (cementite).

The hardness of white cast iron is dependent on the amount of cementite (Fe_3C) in the structure and the cooling rate. In general, as the carbon content increases the hardness increases due to increased amount of cementite in the structure (see Table 2). As the (equilibrium) cooling rate increases the hardness increases due to the decrease in interlamellar spacing (the spacing between the Fe_3C and α-ferrite layers) of pearlite (see Table 2).

Experimental

The broad purpose of the experiments was to investigate the residence time dependent process requirements for the iron nugget process. The experiments involved formation and firing of dried green balls bearing magnetite, coal and limestone in a laboratory-scale resistance box furnace (Fig. 5). Pellets were fired at a furnace temperature of 1,425°C for residence times of 10, 16, 22, 28, 34, 40, 50 and 60 minutes (Anameric and Kawatra, 2004).

Materials and procedure. The iron ore used for production of the pellets was a magnetite concentrate with a particle size of 90% passing 25 μm and containing approximately 5% silica gangue. The coal was a high-volatile bituminous coal ground to pass 150 μm, and the limestone flux was ground to a similar size distribution. A western bentonite was used as binder for the pellets. The mixture used for making dried green balls was as follows:

- 71.84% magnetite (iron source),
- 20% high-volatile bituminous coal (reductant and carbon source),
- 7.5% limestone (flux) and
- 0.66% bentonite (binder).

Table 1 — Chemical composition ranges for typical unalloyed cast irons and blast furnace pig iron.

Element	Blast furnace pig iron, wt%[1]	White cast iron, wt%[2]	Gray iron, wt%[2]	Malleable iron, wt%[2]	Ductile iron, wt%[2]
C	4-5 (saturated)	1.8-3.6	2.5-4.0	2.00-2.60	3.0-4.0
Si	0.3-1	0.5-1.9	1.0-3.0	1.10-1.60	1.8-2.8
S	0.03	0.06-0.2	0.02-0.25	0.04-0.18	<0.03
P	<1	0.06-0.18	0.05-1.0	<0.18	<0.10
Mn	0.1-2.5	0.25-0.80	0.25-1.0	0.20-1.00	0.10-1.00

[1]Peacy and Davenport (1979) [2]Smith (1993)

The experimental procedures for dried green ball, direct reduced iron, transition direct reduced iron and pig iron nugget production are shown in Fig. 5. The analysis techniques used are shown in Fig. 6. These techniques and procedures were described extensively earlier in Kawatra and Ripke (2001) and Anameric and Kawatra (2004).

The physical and chemical analysis procedure for the products was as follows (see Fig. 6):

- *Optical microscopy:* to characterize the nugget microstructure, which identifies the phases and the constituents present and relates it to the known microstructures.
- *Scanning electron microscopy:* for further characterization of the microstructure with accompanying electron dispersive spectroscopy (EDS) of the phases and constituents.
- *Microhardness measurements:* for detection of the bulk carbon content change (1-kg load) (16 measurements were taken on the metallized area) (Krauss, 1990).

Results and discussion

Products. Three chemically and physically different products, i.e., direct reduced iron (DRI), transition direct reduced iron (TDRI) and pig iron nuggets (PIN), were produced. The formation of DRI, TDRI and PIN was dependent on the furnace residence time and corresponding change in the carbon content of the system. As the furnace residence time increases, the amount of carbon diffused in the metal increased, and the melting point of the metallized portion decreases until the eutectic point (4.3% C) was reached (Fig. 3), allowing the iron to melt and resulting in the formation of pig iron nuggets. Figure 7 shows the DRI, TDRI and PIN formed as a function of the residence time at 1,425°C furnace temperature.

Direct reduced iron (DRI): Direct reduced iron (DRI) was produced as a complete solid-state product (Fig. 8 (a), (b) and (c)). After the complete reduction of magnetite to Fe (according to Reactions (9) and (10)), the first metal formed contained

Table 2 — Typical Vickers hardness values for certain iron-carbon alloys (Vander Voort,1999).

Material	HVN
α-ferrite	80
Pearlite (fine interlamellar spacing)	400
Pearlite (coarse interlamellar spacing)	250
Cementite (Fe_3C)	800
Mild steel (0.1-1.2 wt% C)	140

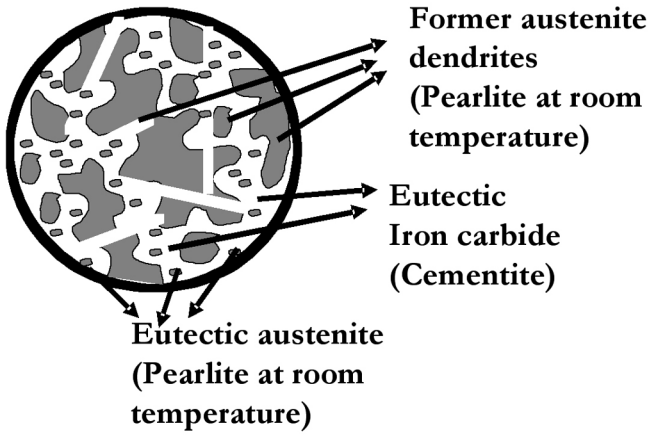

Figure 4 — The schematic representation of the white cast iron microstructure at room temperature. The dark-gray areas represent the former austenite dendrites that transformed to pearlite (the eutectoid microstructure, alternating layers of Fe_3C and α-ferrite), and the white areas represent the eutectic iron carbides (cementite). Cementite is hard, brittle and dominates the microstructure.

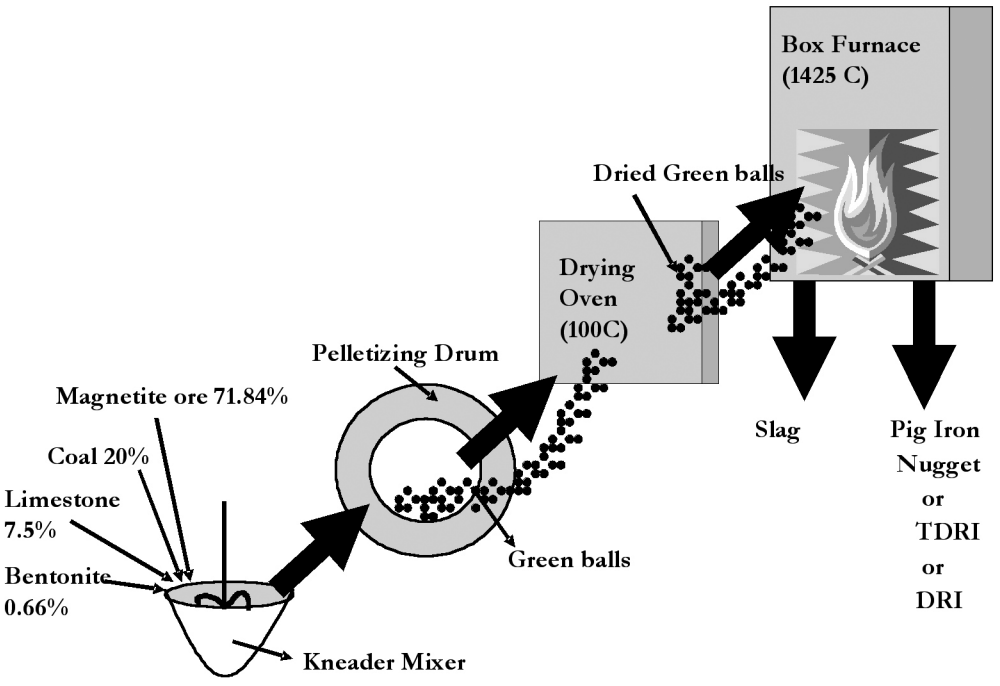

Figure 5 — Schematic drawing of the experimental setup used for direct reduced iron (DRI), transition direct reduced iron (TDRI) and pig iron nugget (PIN) production.

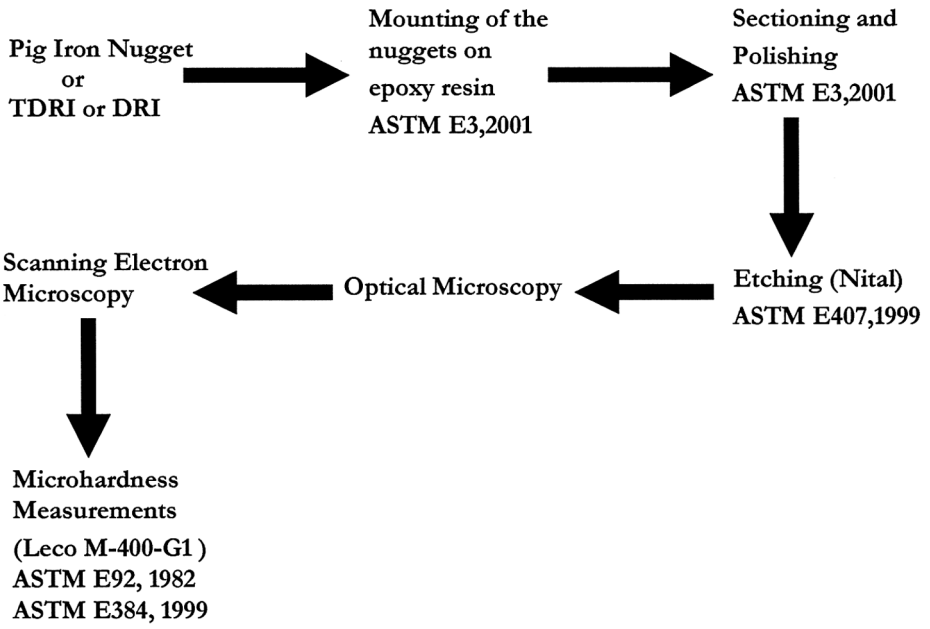

Figure 6 — Schematic drawing of the experimental setup used for the direct reduced iron, transition direct reduced iron and pig iron nugget characterization.

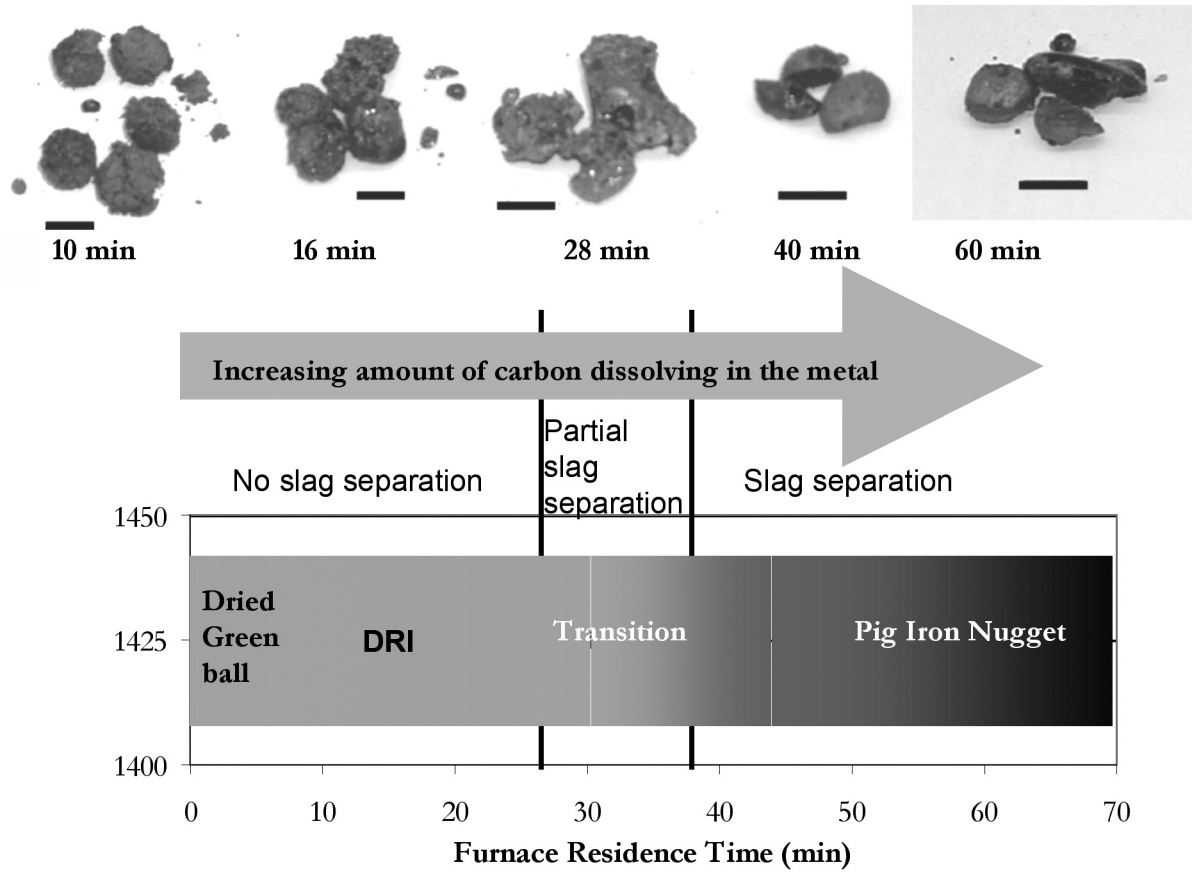

Figure 7 — The summary of the experimental work conducted for determining the residence times required for pig iron nugget making at a furnace temperature of 1,425°C. The pictures of the DRI, TDRI and PIN produced are shown on the top of the figure. The scale bars shown are 10 mm.

little or no carbon and had the structure of solid δ-iron (see Fig. 3). δ-iron on cooling transformed to γ-iron (austenite) and finally to α-ferrite. As the carbon content increased, austenite (γ-iron) would form, which would also transform to α-ferrite/α-ferrite + iron carbide on cooling (see Fig. 3). These solid-state products are called direct reduced iron (DRI). They were produced at residence times 10, 16 and 22 minutes (see Fig. 7). Due to lack of melting of the iron, slag was not separated

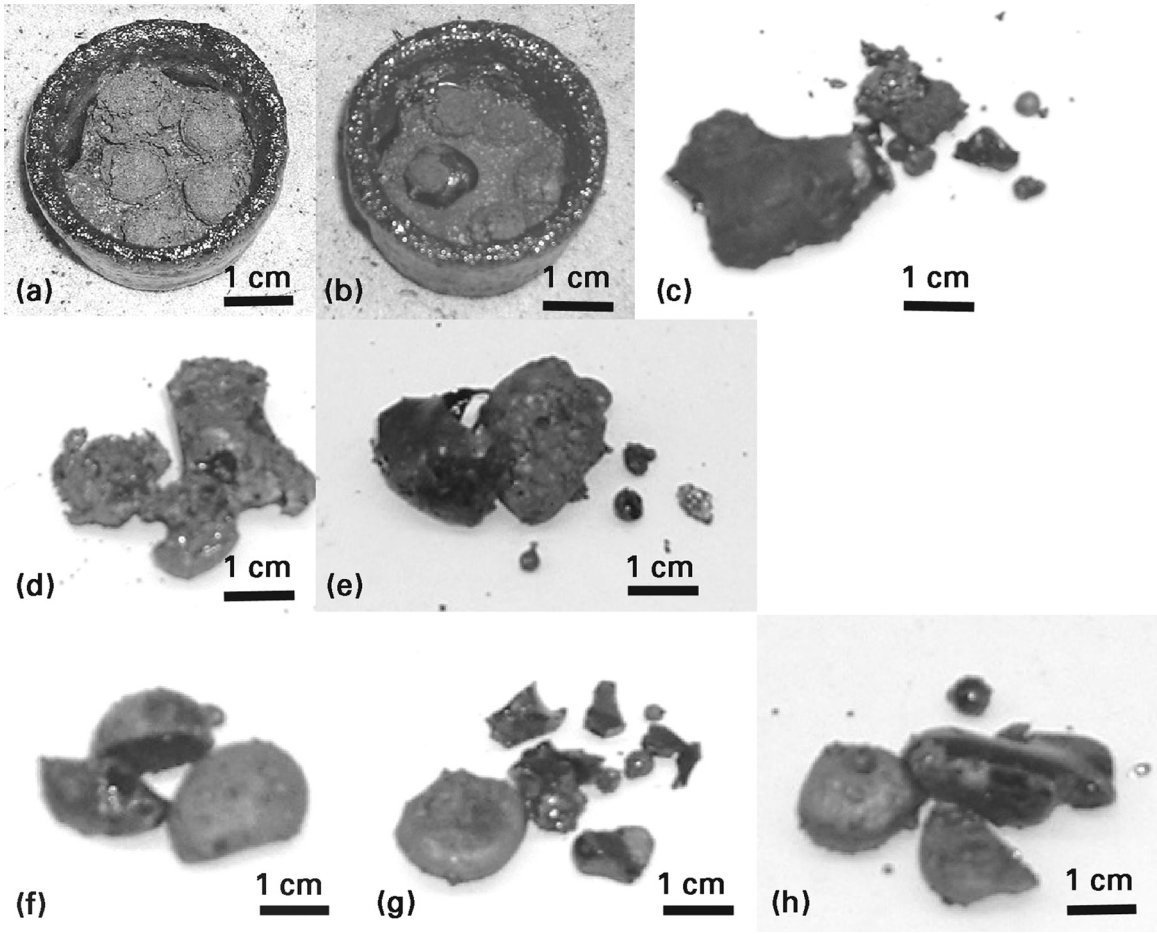

Figure 8 — (a), (b) and (c) show the direct reduced iron (DRI) produced at residence times of 10, 16 and 22 min, respectively. The metallized portion is a solid-state product; slag was not separated from the metal. (d) and (e) show the transition direct reduced iron (TDRI) produced at residence times 28 and 32 min, respectively. The metallized portion is a partially melted solid- and liquid-state product; slag was partially separated from the metal. (f), (g) and (h) show the pig iron nugget (PIN) and slag produced at residence times 40, 50 and 60 min, respectively. The metallized portion is a liquid-state product; slag was completely separated from the metal.

from the metallized portion, resulting in a spongy structure of slag interspersed throughout the metal.

Transition direct reduced iron: After the formation of DRI structure as the carbon concentration increased beyond the austenite solidus (Fig. 3), a mixture of solid and liquid (γ-iron and liquid) formed, and on cooling, austenite (γ-iron) transformed to α-ferrite and cementite. The liquid solidified in a manner to include dendritic austenite (γ-iron) and a eutectic product containing cementite. Liquid and solid-state products are called transition direct-reduced iron (TDRI) (see Fig. 8 (d) and (e)). This was produced at a residence time of 28 minutes (Fig. 7). Due to partial melting, partial slag separation began but was not completed.

Pig iron nuggets: **A f**urther carbon concentration increase (Fig. 3) led to 100% liquid formation, which solidified to form pig iron nuggets upon cooling. These nuggets had the microstructures shown schematically in Fig. 4, which were found to correspond to the microstructures seen in white cast iron. The pig iron nuggets were produced at residence times ≥ 40 minutes (Fig. 7 and Fig 8 (f), (g) and (h) (Anameric and Kawatra, 2004). Complete slag separation was achieved due to complete melting of the metal.

Optical microscopy and scanning electron microscopy results.

Direct reduced iron: The optical micrographs for direct reduced iron (DRI) made at furnace residence times of 16 and 22 minutes are shown in Fig. 9 (a), (b) and (c) and in Fig. 11 (a), (b) and (c), respectively. In these figures the whitest areas represent the metallized portion of the DRI, the light-gray areas (tree like structures) represent the wustite (FeO) dendrites in the slag and the dark-gray areas represent the slag matrix. The FeO contents of the DRI indicated that iron reduction was not yet complete in these samples. The presence of a dendritic structure implies the crystal growth of a phase, in this case wustite, during slow cooling. Both structures (Fig. 9 (a), (b) and (c) and Fig. 11 (a), (b) and (c)) have heterogeneous microstructures including both slag and the metallized material. Morton and Wingrove (1969), Maddin (1975) and Blomgren and Tholander (1986) reported similar slag inclusion microstructures in early ironmaking practices.

For the direct-reduced iron produced at a residence time of 16 minutes, no obvious iron carbides were observed in the metallized portion (Fig. 9 (c)). However, for the direct reduced iron produced at longer residence time of 22 minutes, iron carbides were observed within the metallized portion of

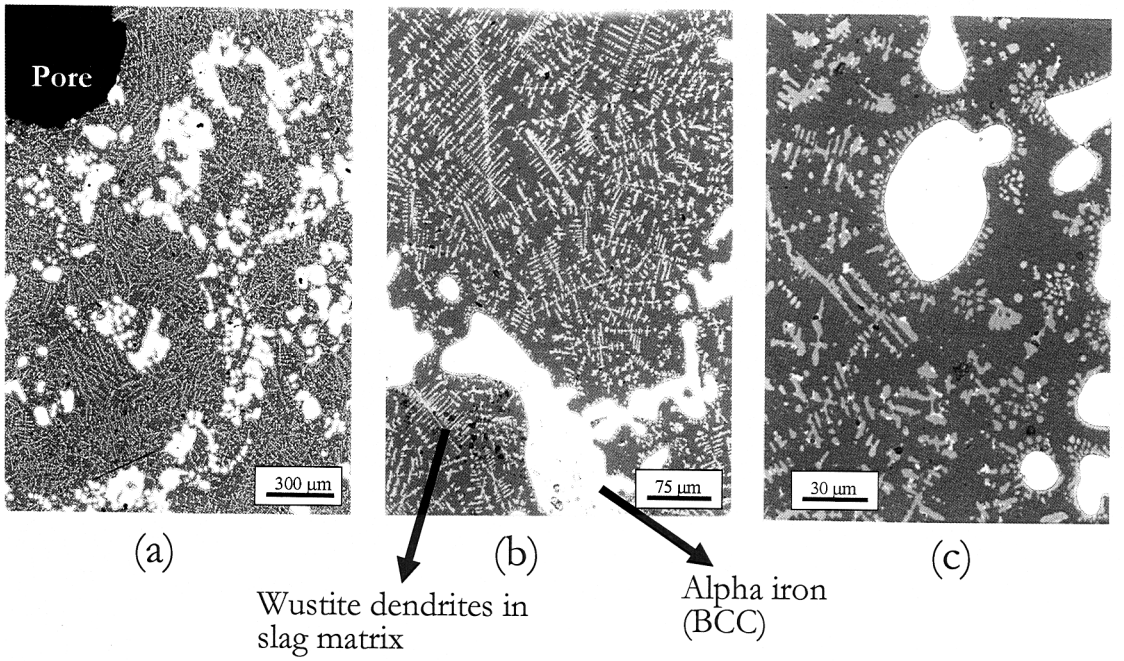

Figure 9 — (a), (b) and (c) are optical micrographs, at various magnifications, of a cross section of a direct reduced iron produced at furnace residence time of 16 min.

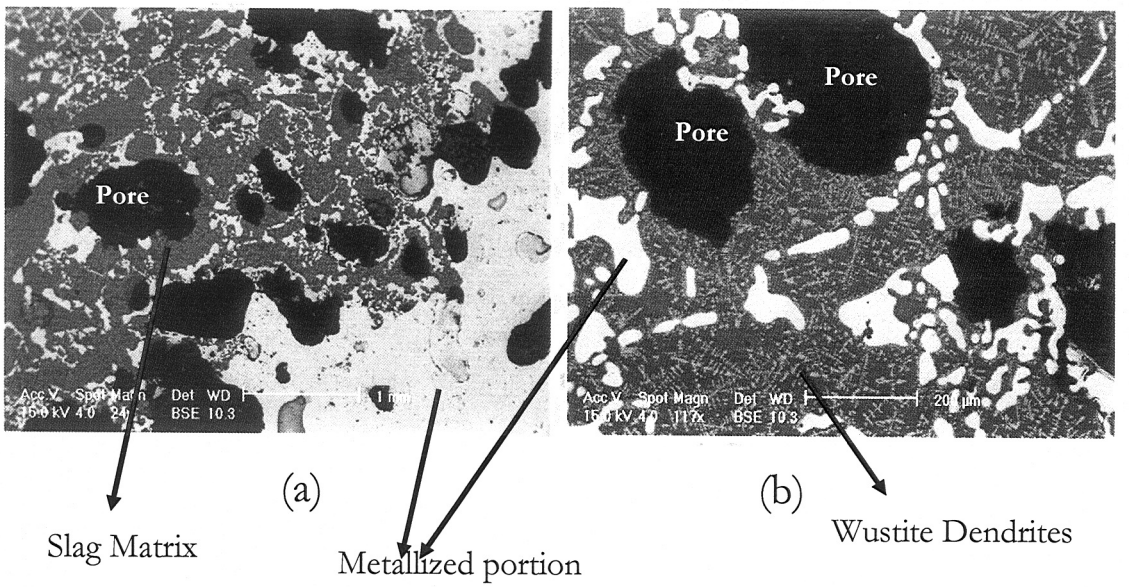

Figure 10 — (a) and (b) are SEM backscattered electron images, at two different magnifications, of the DRI made at a furnace residence time of 16 min.

the microstructure (Fig. 11 (c)). It can be inferred from Fig. 3 that the δ-iron formed at 1,425°C eventually transformed to austenite, as carbon content increased, which then transformed to α-ferrite and cementite during cooling.

Identification of the phases alpha iron, wustite and slag matrix and constituents were made using scanning electron microscopy and local chemical analysis by energy dispersive X-ray spectroscopy (EDS). The backscattered electron image (atomic number contrast) for the DRI produced at 16 minutes of residence time is shown in Fig. 10. The secondary electron image (topographic contrast) for the DRI produced at 22 minutes of residence time is shown in Fig. 12. The phases identified using this method and their approximate chemical compositions are given in Table 3.

Pig iron nuggets: Pig iron nuggets were produced at higher furnace residence times. The optical micrograph of the pig iron nugget made at 1,425°C furnace temperature and 60 minutes furnace residence time is shown in Fig. 13. This microstructure (Fig. 13) was composed of a dendritic pattern of fine pearlite (dark-gray areas) and interdendritic eutectic

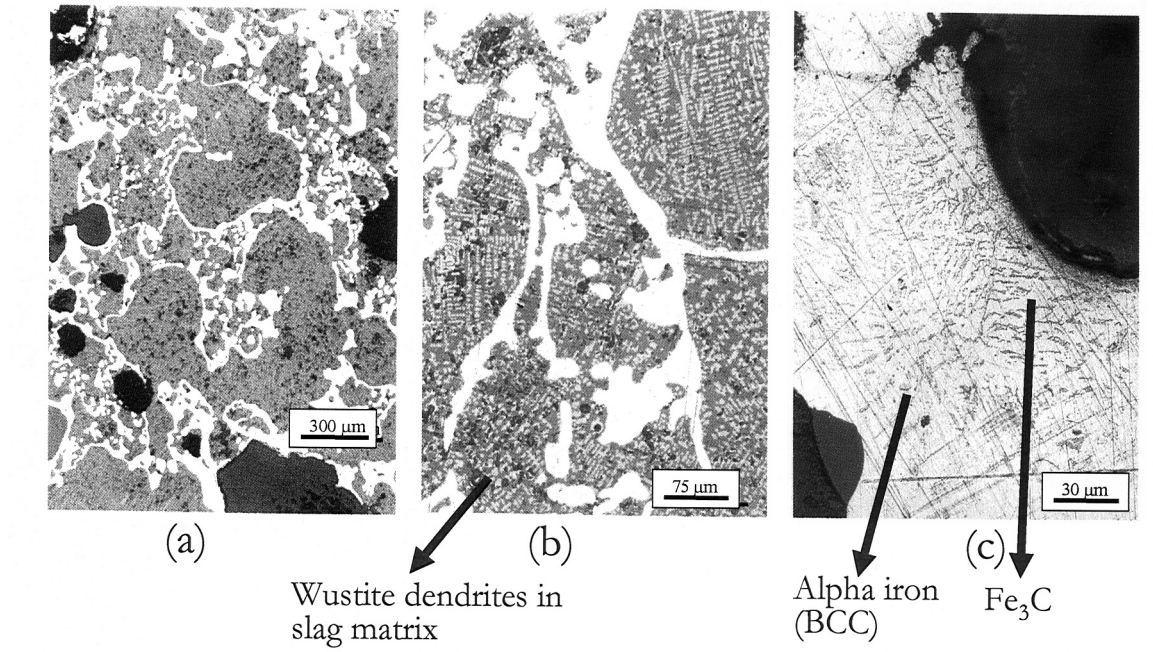

Figure 11 — (a), (b) and (c) are optical micrographs, at various magnifications, of a cross section of a direct reduced iron produced at furnace residence time of 22 min.

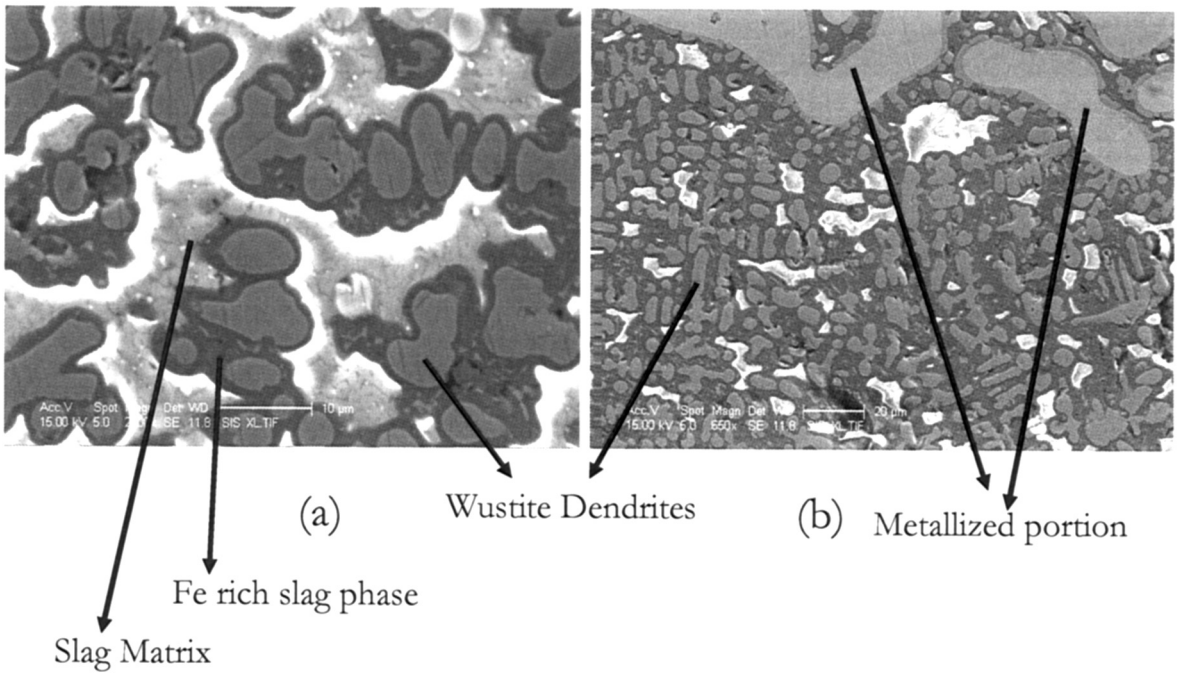

Figure 12 — (a) and (b) are SEM secondary electron images, at two different magnifications, for the DRI made at furnace residence time of 22 min.

mixture of cementite and pearlite (light areas). They were very similar to the white cast iron structure shown in Fig. 4 (Davis, 1990; Smith, 1993; Callister, 1997; Mehl, 1999; Anameric and Kawatra, 2004). It can be seen from Fig. 3 that during cooling molten pig iron nuggets first transformed into dendrites of austenite while passing through the γ-Fe/liquid phase field. Subsequently, this proeutectic austenite transformed to pearlite (alternating layers of iron carbide (Fe_3C) and α-ferrite). In addition, when 1,147°C was reached, any remaining liquid solidified into a eutectic morphology consisting of austenite (transforms to pearlite upon cooling) and iron carbide (Fe_3C). Iron carbide appears to have penetrated the pearlite (transformed austenite) (Heine and Barton, 1977; Park and Verhoeven, 1996; Radzikowska and Voort, 1998; Mampaey, 2001).

Microhardness measurements. The Vickers hardness measurements (1-kg load) (ASTM E 92-82, 1997 and ASTM E 384, 1999) on the metallized portion were taken to detect the increase in the cementite (iron carbide) amount in the micro-

Table 3 — The approximate local chemical analysis of the wustite, Fe-rich slag phase and α-Fe present in the DRI (production furnace residence time 22 min) microstructure.

Element	Wustite (FeO) dendrites, %	Fe-rich slag phase, %	α -Fe (metallized portion of the DRI), %
Fe	72.58	31.31	99.9
C	5.39	3.76	0.1
O	21.29	29.46	–
Si	0.42	15.87	–
P	0.10	0.51	–
S	0.22	0.59	–
Mg	–	1.28	–
Al	–	1.62	–
Ca	–	15.61	–

Table 4 — The average Vickers hardness values of the DRI, TDRI and PIN made at various furnace residence times. 16 or more measurements were taken for each sample.

Furnace temperature, °C	Furnace residence time, min	HVN	Standard deviation
1,425	10	90.6	27.4
1,425	16	75.1	27.1
1,425	22	124.3	20.0
1,425	28	132.7	23.4
1,425	30	307.8	21.1
1,425	34	308.7	15.7
1,425	40	351.1	25.8
1,425	50	399.7	27.2
1,425	60	412.4	53.8

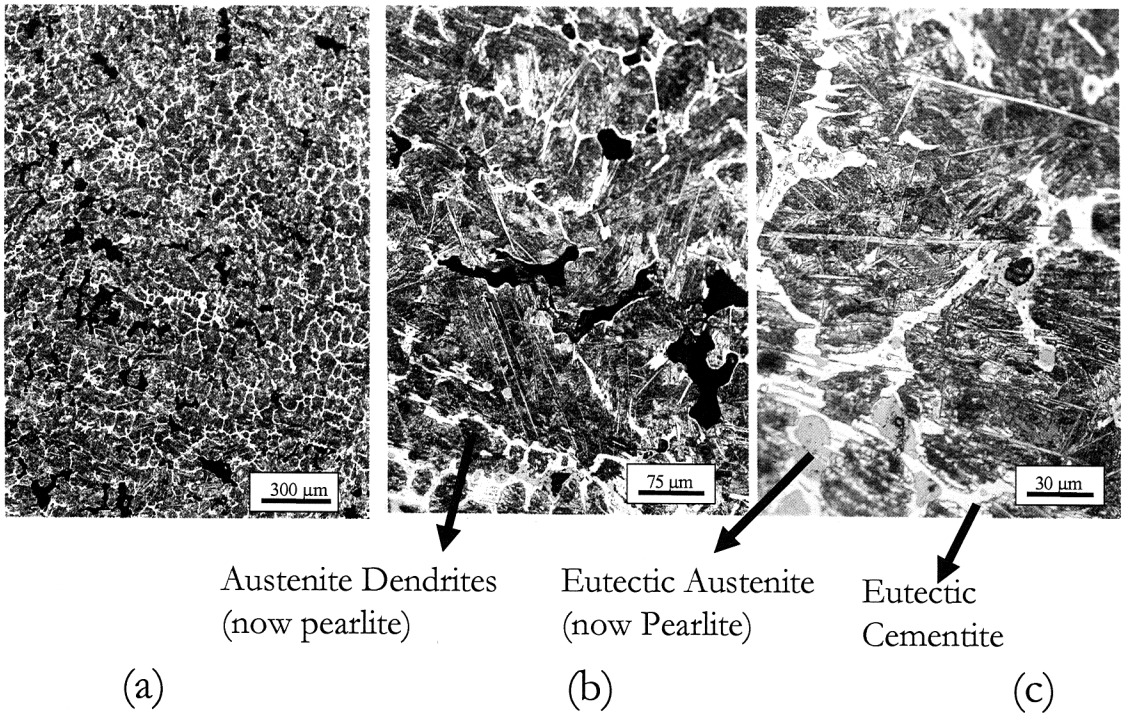

Figure 13 — (a), (b) and (c) are optical micrographs at varying magnifications of a cross section of a pig iron nugget produced at furnace residence time 60 min.

structure with increasing furnace temperature and/or residence time, because the Vickers hardness increases with increasing amounts of dissolving carbon in the metallized portion (amount of carbides) (Krauss, 1990).

The average Vickers hardness values of the DRI, TDRI and PIN made at varying furnace temperatures and residence times is summarized in Fig. 14 and Table 4. The microhardness of the DRI produced varied from 60 to 120 HVN. The microhardness of the TDRI produced varied from 120 to 325 HVN. The microhardness of the pig iron nuggets produced varied from 325 to 420 HVN. The increase in the microhardness with increasing furnace temperature and residence time is shown in Fig. 14. Also shown are the hardness ranges.

There are two types of iron carbides contributing to the microhardness of the structure. The first type consists of those formed by solid-state reactions, and the second type consists of those that form by liquid-state reactions. Solid-state iron carbides were formed in DRI and in available solid-state reacting sites in TDRI. Cementite was formed in available liquid-state reacting sites in TDRI and in pig iron nuggets. The diffusion of carbon in the solid state is much slower than in the liquid state. Therefore, the large increase in hardness from DRI to TDRI and to pig iron nuggets (Fig. 14) was due to more and/or rapid diffusion of carbon in the metallized portion. In other words, it was due to increasing amounts of eutectic cementite with increasing furnace residence time.

Conclusions

Three chemically and physically distinct products were produced as a function of furnace residence time after the

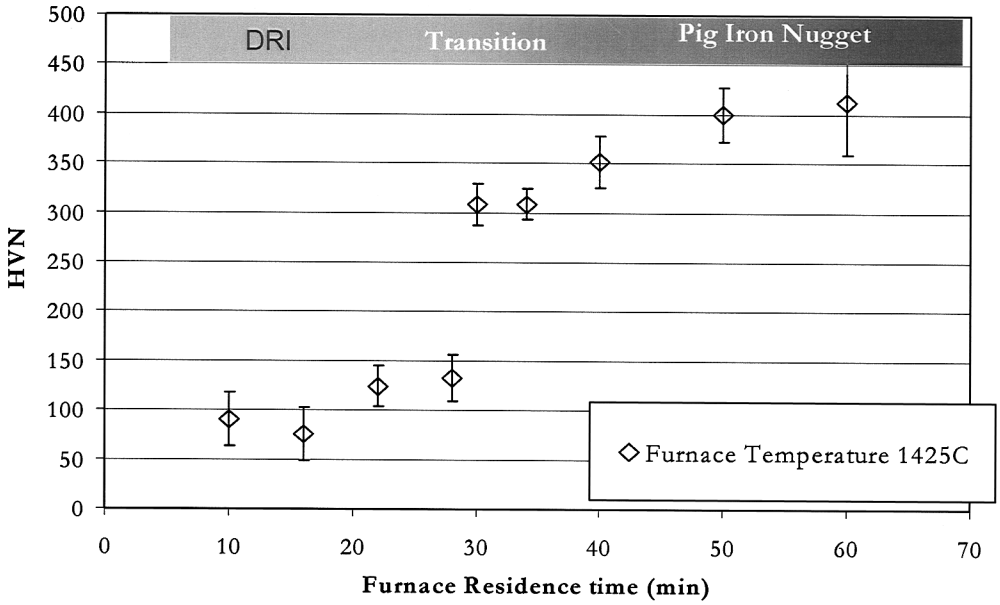

Figure 14 — The average Vickers hardness values of the DRI, TDRI and PIN representing the increase in the amount of carbon in the system. Sixteen or more measurements were taken from the metallized portion of each sample.

reduction of magnetite to iron. In this study the temperature of the furnace was kept constant at 1,425°C, but the residence times were varied. As the furnace residence time increased, the amount of carbon diffused into the metal increased, lowering the melting point of the metal phase. The three products were:

- *Direct reduced iron (DRI):* solid-state product with no slag separation.
- *Transition direct reduced iron (TDRI):* liquid- and solid-state products with partial slag separation.
- *Pig iron nuggets (PIN):* liquid-state products with complete slag separation, high iron yield.

Carburization was necessary to liquefy and consolidate the metal, allowing the slag to separate from the structure and transforming DRI into TDRI and finally in to pig iron nugget. Carbon diffusion and the production of liquid-state products are critical for producing a high-grade product comparable to blast furnace pig iron. Therefore, sufficient processing time must be allowed for this diffusion of carbon to occur.

The pig iron nuggets were not instantaneously produced, and DRI did not transform directly into the pig iron nuggets. The transition stage and the kinetics of the transition reactions, carburization rate control is important for the production of uniform quality and carbon content pig iron nuggets. In addition, the determination of whether carburization or, as stated in the literature, wustite reduction, or reducing agent generation is the rate controlling step should be investigated for future process development. Thus, this would help larger-scale testing and production operations.

Acknowledgments

This work was partially supported by the U.S. Department of Energy Mining Industry of the Future Program under Grant No. DE-FC26-03NT41924. The assistance of Dr. Timothy Eisele of Michigan Tech is also gratefully acknowledged.

References

Anameric, B., and Kawatra, S.K., 2004, "A Laboratory study relating to the production and properties of pig iron nuggets," Paper 04-098, presented at the SME Annual Meeting, Feb. 3-25, 2004, Denver, Colorado, Metallurgical Process Fundamentals: Pyrometallurgical Processing Session.

Abraham, M.C., and Gosh, A., 1979, "Kinetics of reduction of iron oxide by carbon," *Ironmaking and Steelmaking*, Vol. 6, pp. 14-23.

Agrawal, B.B., Prasad, K.K., Sarkar, S.B., and Ray, H.S., 2000, "Cold bonded ore-coal composite pellets for sponge iron making, Part 1. Laboratory Scale Development," *Ironmaking and Steelmaking*, Vol. 27, Part 6, pp. 421-425.

ASTM E 3, 2001, "Standard Guide for Preparation of Metallographic Specimens," *Annual Book of ASTM Standards*, Vol. 03.01 (Metals Test Methods and Analytical Procedures, Metals, Mechanical testing, elevated and Low-temperature Tests, Metallography), pp. 1-11.

ASTM E 92-82, 1997, "Standard Test Method for Vickers Hardness of Metallic Materials," *Annual Book of ASTM Standards*, Vol. 03.01 (Metals Test Methods and Analytical Procedures, Metals, Mechanical testing, elevated and Low-temperature Tests, Metallography), pp. 229-237.

ASTM E 384, 1999, "Standard Test Method for Microindentation Hardness of Materials," *Annual Book of ASTM Standards*, Vol. 03.01 (Metals Test Methods and Analytical Procedures, Metals, Mechanical testing, elevated and Low-temperature Tests, Metallography), pp. 418-427.

ASTM E 407, 1999, "Standard Practice for Microetching Metals and Alloys," *Annual Book of ASTM Standards*, Vol. 03.01 (Metals Test Methods and Analytical Procedures, Metals, Mechanical testing, elevated and Low-temperature Tests, Metallography), pp. 474-493.

Blomgren, S., and Tholander, E., 1986, "Influence of the ore smelting course on the slag microstructures at early ironmaking, usable as identification basis for the furnace process employed," *Scandinavian Journal of Metallurgy*, Vol. 15, pp. 151-160.

Callister, W.D., 1997, *Materials Science and Engineering, An Introduction*, 4th Edition, John Wiley and Sons, Inc.

Chatterjee, A., 1994, *Beyond the Blast Furnace*, CRC Press, Inc.

Davis, J.R., 1990, *Metals Handbook, Properties and Selection: Irons, Steels, and High Performance Alloys*, ASTM International, 10th Edition, Vol. 1, pp. 93.

Fruehan, R.J., 1977, "The rate of reduction of iron oxides by carbon," *Metallurgical and Materials Transactions B*, Vol. 8, pp. 279-286.

Ghosh, P.C., and Tiwari, S.N., 1970, "Reduction of pellets of iron ore plus lignite coke," *ISIJ International*, Vol. 208, pp. 255-257.

Goksel, M.A., 1977, "Fundamentals of cold bond agglomeration processes," *Agglomeration 77*, Vol. 2, AIME, New York, pp. 877-900.

Goksel, A., Coburn, J., and Kohut, J., 1991, "Recycling waste oxide from iron-steel plants using the PTC process," *Ironmaking Conference Proceedings*, Vol. 50, Washington, DC, April 14-17, 1991, pp. 97-112.

Goksel, A., Scott, T.A., Weiss, F., and Coburn, J., 1988, "PTC-Cold Bond Agglomeration Process and its various applications in the iron and steel industry," *Institute for Briquetting and Agglomeration, 20th Biennial Conference*, Vol. 20, Orlando, Florida, Sept. 1987, pp. 191-213.

Haque, R., and Ray, H.S., 1995, "Communication: role of ore/carbon contact and direct reduction in the reduction of iron oxide by carbon," *Metallurgical and Materials Transactions B*, Process Metallurgy and Materials Processing Science, Vol. 26, No. 2, pp. 400.

Heine, R.W., and Barton, J.E., 1977, "Eutectic solidification of white iron and its effects on malleable iron castings," *Transactions of the American Foundarymen's Society*, Vol. 85, pp. 379-388.

Kawatra, S.K., and Ripke, S.J., 2001, "Developing and understanding the bentonite fiber bonding mechanism," *Minerals Engineering*, Elsevier Press, Vol. 14, No. 6, pp. 647-659.

Krauss, G., 1990, *Microstructures, Processing and Properties of Steels, Metals Handbook, Properties and Selection: Irons, Steels, and High Performance Alloys*, ASTM International, 10th edition, Vol. 1, pp. 126, 127, 132.

Maddin, R., 1975, "Early iron metallurgy in the near east," *Transactions of the Iron and Steel Institute of Japan*, Vol. 15, No. 2, pp. 38-68.

Mampaey, F., 2001, "Cast Iron, Div. 5 – Solidification morphology of white cast iron," *Transactions of the American Foundarymen's Society*, Vol. 109, pp. 1049-1059.

Mehl, F.R., 1999, *Microstructure of Cast Irons, Metals Handbook, Atlas of Microstructures of Industrial Alloys*, ASTM International, 8th Edition, Vol. 7, pp. 95,99.

Mourao, M.B., and Capacchi, J.D.T., Sept-Dec 1996, "Rate of reduction of iron oxide in carbon-bearing pellets," *Transaction of the Institute of Mining and Metallurgy*, Vol. 105, C 151-204, pp. 190-196.

Morton, G., and Wingrove, J., 1969, "Constitution of bloomery slags: Part I: Roman," *Journal of The Iron and Steel Institute*, Vol. 207, Part 12, pp. 1556-1969.

Nascimento, R.C., Mourao, M.B., and Capocchi, J.D.T., 1997, "Microstructures of self-reducing pellets bearing iron ore and carbon," *ISIJ International*, Vol. 37, No. 11, pp. 1050-1056.

Nascimento, R.C., Mourao, M.B., and Capocchi, J.D.T., 1998, "Reduction-swelling behavior of pellets bearing iron ore and charcoal," *Canadian Metallurgical Quarterly*, Vol. 37, No. 5, pp. 441-448.

Nascimento, R.C., Mourao, M.B., and Capocchi, J.D.T., 1999, "Kinetics and catastrophic swelling during reduction of iron ore in carbon bearing pellets," *Ironmaking and Steelmaking*, Vol. 26, No. 3, pp. 182-186.

Park, J.S., and Verhoeven, J.D., 1996, "Directional solidification of white cast iron," *Metallurgical and Materials Transactions A*, Vol. 27A, No. 8, pp. 2328-2337.

Rao, Y.K., 1971, "The kinetics of reduction of hematite by carbon," *Metallurgical and Materials Transactions*, Vol. 2, pp. 1439-1447.

Peacey, J.G., and Davenport, W.G., 1979, *The Blast Furnace Theory and Practice*, Pergamon Press, 1st Edition.

Radzikowska, J., and Voort, G.V., 1998, "The basics of cast iron metallography," *Modern Casting*, pp. 46-48.

Seaton, C.E., Foster, J.J., and Velasco, J., 1983, "Reduction kinetics of hematite and magnetite pellets containing coal char," *ISIJ International*, Vol. 23, pp. 490-496.

Smith, W.F., 1993, *Structure and Properties of Engineering Alloys*, McGraw-Hill Materials Science and Engineering Series, 2nd Edition, pp. 1-41, 82.

Srinivasan, N.S., and Lahiri, A.K., 1977, "Studies in the reduction of hematite by carbon," *Metallurgical and Materials Transactions B*, Vol. 8, pp. 175-178.

Vander Voort, G.F., 1999, *Metallography, Principles and Practice*, ASM International, Materials Park, Ohio.

Zervas, T., McMullan, J.T., and Williams, B.C., 1996a, "Direct smelting and alternative processes for the production of iron and steel," *International Journal of Energy Research*, Vol. 20, pp. 1103-1128.

Zervas, T., McMullan, J.T., and Williams, B.C., 1996b, "Developments in iron and steel making," *Int. Journal of Energy Research*, Vol. 20, pp. 69-91.

Zervas, T., McMullan, J.T., and Williams, B.C., 1996c, "Solid-based processes for the direct reduction of iron," *International Journal of Energy Research*, Vol. 20, pp. 255-278.

Zervas T., McMullan J.T., and Williams B.C., 1996d, "Gas-based direct reduction processes for iron and steel production," *International Journal of Energy Research*, Vol. 20, pp. 157-185.